ELSEVIER

Journal of Nuclear Materials 271&272 (1999) 102–105

journal of nuclear materials

Influence of post-irradiation thermal annealing on the mechanical properties of ion irradiated layers in 316L stainless steel

C. Robertson *, L. Boulanger, S. Poissonnet

Section de Recherches de Métallurgie Physique, Direction des Technologies Avancées, Commissariat à l'Energie Atomique, Centre d'Etudes de Saclay, 91191 Gif-sur-Yvette, France

Abstract

Irradiation-induced modification of the mechanical properties of metals is an important but poorly understood technological problem, involving microscopic phenomenon upon which the present study concentrates. In an attempt to take advantage of charged particles irradiation, we applied a combination of transmission electron microscopy (TEM) and sub-micron indentation technique to ion-irradiated layers of 316L steel specimens, irradiated with krypton ions up to 3 dpa at 350°C. It was found that hardness as measured on the ion-irradiated zone is modified by post-irradiation thermal annealing and that the amplitude of this modification is important at 600°C.

1. Introduction

316L steel is one of the main candidate for first wall metallic structures of near-term fusion reactors. However, it is now a well-established fact that neutron irradiation results in substantial alteration of the macroscopic deformation behavior of metallic alloys [1–5], which could in turn affect long-term reliability and maintenance costs of fusion reactors. Irradiation-induced increase in the upper tensile yield stress is one extensively studied effect, which is usually explained in terms of conventional disperse barrier hardening models. According to these models, microstructural defects produced by high energy cascades are assumed to act as obstacles to gliding of dislocation in their respective slip planes.

Our goal in this work has been to attempt to clarify the nature of such mesoscopic scale obstacles, using a combination of ion irradiation, nano-indentation and post-irradiation thermal annealing. While the use of heavy ion beams usually results in irradiated layer thickness that are very small (< 1 μm), it nevertheless avoids many other operational difficulties (activation, low damage creation rate, etc.). Besides, mesoscopic scale mechanical properties of such layers can still be assessed by means of nano-indentation testing [6,7], whereby sub-micron plastic deformation and measurements of local hardness are simultaneously performed. Nano-hardness measurements have been recorded onto individual irradiated specimens, both prior to and after thermal annealing. Because thermal annealing modifies crystalline microstructures in general (including irradiation-induced defects), the evolution of hardening with annealing temperature should then be related to the stability of the irradiation defects that interact with moving dislocations, if conventional disperse barrier hardening models are correct. Therefore, the evolution of hardening with annealing temperature should provide insights about the nature of the irradiation defects that are genuinely responsible for hardening phenomenon.

2. Experimental

The specimens studied here are 316LN steel disks, with a composition and preliminary preparation as described elsewhere [7]. The three specimens were all

* Corresponding author. Fax: +33-1 69 08 68 67; e-mail: roberts@srmp101.saclay.cea.fr

0022-3115/99/$ – see front matter
PII: S0022-3115(98)00768-5

Table 1
User-selected indentation parameters

Loading rate (mN/s)	0.14
Max. depth (nm)	100
Distance between indents (μm)	50
Analysis method	Oliver and Pharr

together exposed to a 1200 keV krypton ion beam generated by a van de Graaff accelerator, up to 3 dpa at 350°C. It is worth mentioning that the specimen holder is so designed that only the inner part of the disks is exposed to the beam, while the outer part is hidden and therefore serves as a reference specimen. As the indenter is driven into and withdrawn from the sample according to the parameters as indicated in Table 1, a load versus indenter displacement curve is recorded, from which local nano-hardness is deduced [6,7].

Arrays formed of identical indentations were first made on both inner and outer parts of each disk (in other words, onto ion-irradiated and reference materials, respectively), in order to evaluate the amplitude of initial irradiation-induced hardening. The systematic use of the outer disk part as a reference specimen avoided inhomogeneities between different specimens and thermal variations during ion implantation from affecting the interpretation of the results. Next, the disks were separately annealed, each at a distinct temperature for 1 h (at 350°C, 500°C and 600°C, respectively), following which, additional outer and inner indentation arrays were made, using the same indentation parameters as before. The 'new' post-annealing hardness values were then compared to the pre-annealing ones, for each specimen. Finally, a TEM thin foil was prepared using back side electropolishing method, whereby the irradiated (and indented) side was coated with an easily removed lacquer.

3. Results

3.1. Nano-indentation

3.1.1. As irradiated

On the three irradiated specimens labeled 1, 2 and 3, an irradiation-induced relative hardening $\Delta H/H$ of about 10% was reproducibly observed (Fig. 1) though with some dispersion. Note that $\Delta H = (H_{in} - H_{out})$ and that both H_{in} and H_{out} are mean values computed from more than 40 individual hardness values h obtained by the analysis of as many individual indent curves. The selected analysis method was Oliver and Pharr's [6]. The error bars correspond to 2 times the standard error on $\Delta H/H$.

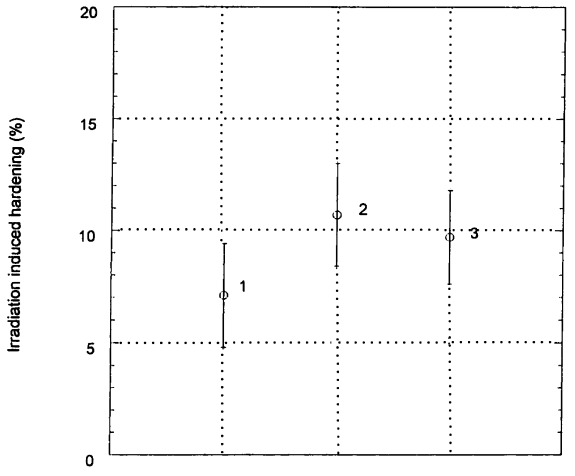

Fig. 1. Relative irradiation-induced hardening in the three irradiated samples.

3.1.2. After thermal annealing

If one compares Fig. 1 with Fig. 2, it can be shown that while irradiation-induced hardening $\Delta H/H$ was not significantly reduced following thermal annealing at 350°C, it was almost eliminated after similar treatment at 600°C. On the other hand, 350°C and 500°C thermal annealing yielded no significative change on $\Delta H/H$ values. From the data, it can be shown that post-irradiation thermal annealing affects the amplitude of $\Delta H/H$, depending on the annealing temperature. Note that the results presented in Fig. 2 come from the analysis of more than 40 individual indentation curves.

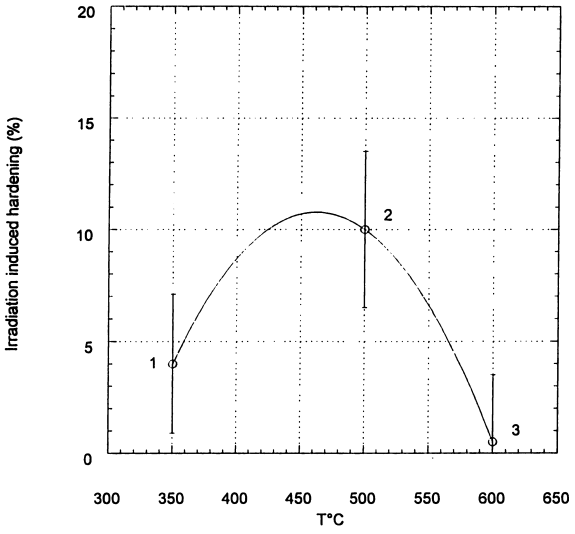

Fig. 2. Relative irradiation-induced hardening $\Delta H/H$ after annealing at 350°C, 500°C and 600°C.

3.2. TEM observations

3.2.1. As irradiated

On all specimens examined here, the main irradiation-induced features visible by TEM (Fig. 3) consist of a homogeneous distribution of defect clusters having apparent diameters ranging 2–4 nm. TEM stereographic views show that the defect clusters are located within a thin layer beneath the irradiated surface only. In addition, given that the foil thickness smoothly increases from the edges towards the thicker regions, the number of clusters regarding distance (with respect to the foil edge) becomes constant at a distance corresponding to a foil thickness of about 250 nm. It is therefore concluded that the visible clusters are all located within an approximately 250 nm thick surface layer, as predicted by TRIM simulations.

3.2.2. After thermal annealing

The diameter reported in Table 2 is defined as the length perpendicular to the black and white contrast. Nevertheless, the actual cluster size is certainly smaller than the apparent size, because TEM contrast associated with one defect cluster results from the displacement field it creates into surrounding perfect crystal. TEM observations showed that the mean cluster diameter was not noticeably dependent on the annealing temperature (Table 2). The cluster density ρ was computed in two steps. First the number of dislocation loop N per unit area A was evaluated on several TEM micrographs. The volume of material V corresponding to that unit area is A times the foil thickness t, which was obtained by means of TEM fringe technique. Thus, ρ corresponds to (N/V). Lastly, it is found that only the total defect cluster density corresponding to the 600°C anneal differs significantly from that in two others (Table 2).

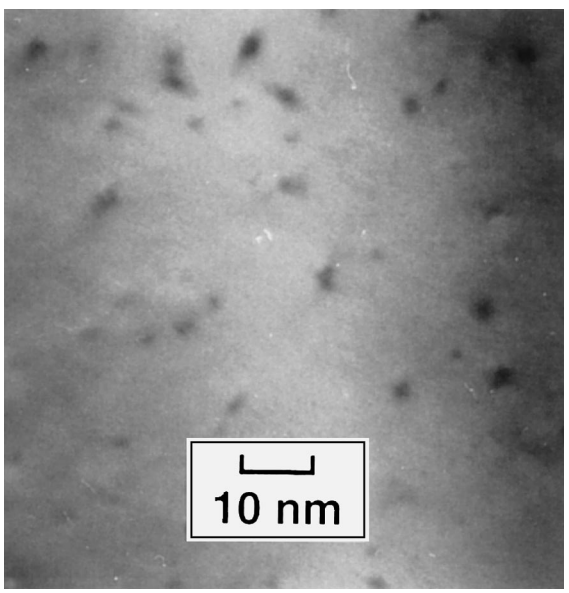

Fig. 3. TEM micrograph of typical irradiation-induced defect clusters after irradiation to 3 dpa at 350°C.

4. Discussion and conclusions

To a fair approximation, provided the indenter penetration depth is not too small, indentation hardness h of most metals can be directly related to their uniaxial tensile yield stress Y_0 [8] by

$$h \approx 3Y_0. \tag{1}$$

According to data from the literature, irradiation of 0.5 dpa at 227°C with fission neutron produce an increase of the tensile yield strength of about 100% [9]. Therefore, considering Eq. (1) and the irradiation conditions as described in Section 2, we would expect hardening of about the same order of magnitude as that of the yield strength increase reported in Ref. [9]. Nevertheless, the measured irradiation-induced hardening of Section 3.1.1 was about an order of magnitude smaller. One cause for the observed discrepancy can come from the indent-induced plastic zone being larger than the damage zone. However, according to ongoing TEM observations and indentation measurements on thinner damage zones [7], the observed discrepancy is more likely to be due to genuine size effects associated with the particular nature of nano-indentation testing, like dislocation nucleation mechanisms and surface effects. Although small, the observed hardening effect is nevertheless very reproducible, indicating that mesoscopic scale mechanisms similar to those predicted by conventional disperse barrier hardening models might somehow take place within the deformed damage zone.

The important effect reported here is that irradiation-induced hardening almost vanished following a post-irradiation thermal annealing at 600°C, in spite of a remnant high density of TEM resolved defect clusters (see Section 3.2). In an attempt to explain this effect, we point out that it is likely that TEM unresolved clusters of vacancies and/or interstitials (also known as residues of displacement cascades) are generated whenever energetic ions collide with cc or fcc crystal lattices, as in 316L steel [10–12]. The presence of such unresolved defects should affect the complex movement of dislocations within the damage zone deformed by the indenter and therefore contributes to the measured irradiation-induced hardening [7]. Considering that the size of the residues of displacement cascades is much smaller than that of the TEM resolved defect clusters reported here, the former would then be much more readily removed than the latter during annealing at 600°C [13,14]. This could explain why irradiation-induced nano-hardening

Table 2
Distribution of defect clusters after annealing

	Defect cluster density ρ and cluster diameter D
Specimen 1 (350°C annealed)	$\rho = (11.0 \pm 1.5) \times 10^{21}$ m^{-3} 1 nm $\leqslant D \leqslant$ 4 nm
Specimen 2 (500°C annealed)	$\rho = (11.3 \pm 1.1) \times 10^{21}$ m^{-3} 1 nm $\leqslant D \leqslant$ 4 nm
Specimen 3 (600°C annealed)	$\rho = (5.9 \pm 1.5) \times 10^{21}$ m^{-3} 1 nm $\leqslant D \leqslant$ 4 nm

vanished following thermal annealing at 600°C, in spite of the quite high density of remnant TEM resolved defect clusters.

Further works to elucidate precisely how temperature affects the dimensional stability of small defects and to determine how strong displacement cascade residues interact with moving dislocations are now in progress.

Acknowledgements

Authors wish to thank Mr G. Martin for his helpful suggestions as well as Mr Y. Serruys for the operation of the van de Graaff accelerator and the TRIM simulations.

References

[1] F.A. Garner, in: R.W. Cahn, P. Haasen, E.J. Kramer (Eds.), Materials Science and Technology, VCH, New York, 1994, p. 419.
[2] N. Yoshida, H.L. Heinish, T. Muroga, K. Araki, M. Kiritani, J. Nucl. Mater. 179–181 (1991) 1078.
[3] M.L. Grossbeck, P.J. Maziasz, A.F. Rowcliffe, J. Nucl. Mater. 191–194 (1992) 808.
[4] R.H. Jones, E.R. Bradley, D.L. Styris, J. Nucl. Mater. 116 (1983) 297.
[5] M. Suzuki, A. Sato, T. Mori, J. Nakagawa, N. Yamamoto, H. Shiraishi, Philos. Mag. A 65 (1992) 1309.
[6] W.C. Oliver, G.M. Pharr, J. Mater. Res. 7 (1992) 1564.
[7] C. Robertson, S. Poissonnet, L. Boulanger, J. Mater. Res. 13(8) (1998) 213.
[8] D. Tabor, Philos. Mag. A 74 (5) (1996) 1207.
[9] M.I. de Vries, in: J.G. Van der Laan (Ed.), ECN (Petten) Rept. ECN-C-90-041, 1990, p. 66.
[10] D.J. Bacon, A.F. Calder, F. Gao, V.G. Kapinos, S.J. Wooding, Nucl. Instrum. Meth. B 102 (1995) 58.
[11] N.V. Doan, R. Vascon, Radiat. Eff. Def. Solids 141 (1997) 363.
[12] N.V. Doan, R. Vascon, Nucl. Instrum. Meth. B 135 (1998) 207.
[13] F.A. Garner, D.S. Gelles, J. Nucl. Mater. 159 (1988) 286.
[14] F.A. Garner, J. Nucl. Mater. 205 (1993) 84.